A *BESS* Sizing Strategy for Primary Frequency Regulation Support of Solar Photovoltaic Plants

Diego Mejía-Giraldo [1,*] ，**Gregorio Velásquez-Gomez** [2] ，**Nicolás Muñoz-Galeano** [1] ，
Juan Bernardo Cano-Quintero [1] and **Santiago Lemos-Cano** [2]

1   Grupo en Manejo Eficiente de la Energía (GIMEL), Departamento de Ingeniería Eléctrica, Universidad de Antioquia (UdeA), Calle 70 No. 52-21, Medellín 050010, Colombia; nicolas.munoz@udea.edu.co (N.M.-G.); bernardo.cano@udea.edu.co (J.B.C.-Q.)
2   Empresa de Energía del Pacífico S.A. E.S.P (EPSA)-Celsia S.A. E.S.P, Carrera 43A No. 1 sur-143, Medellín 050021, Colombia; gvelasquezg@celsia.com (G.V.-G.); slemos@celsia.com (S.L.-C.)
*   Correspondence: diego.mejia@udea.edu.co; Tel.: +57-4-2195-555

Abstract: This paper proposes a strategy for sizing a battery energy storage system (*BESS*) that supports primary frequency regulation (*PFR*) service of solar photo-voltaic plants. The strategy is composed of an optimization model and a performance assessment algorithm. The optimization model includes not only investment costs, but also a novel penalty function depending on the state of charge (*SoC*). This function avoids the existence of a potential inappropriate *SoC* trajectory during *BESS* operation that could impede the supply of *PFR* service. The performance assessment algorithm, fed by the optimization model sizing results, allows the emulation of *BESS* operation and determines either the success or failure of a particular *BESS* design. The quality of a *BESS* design is measured through number of days in which *BESS* failed to satisfactorily provide *PFR* and its associated penalization cost. Battery lifetime, battery replacements, and *SoC* are also key performance indexes that finally permit making better decisions in the election of the best *BESS* size. The inclusion of multiple *BESS* operational restrictions under *PFR* is another important advantage of this strategy since it adds a realistic characterization of *BESS* to the analysis. The optimization model was coded using GAMS/CPLEX, and the performance assessment algorithm was implemented in MATLAB. Results were obtained using actual frequency data obtained from the Colombian power system; and the resulting *BESS* sizes show that the number of *BESS* penalties, caused by failure to provide *PFR* service, can be reduced to zero at minimum investment cost.

1. Introduction

One of the most challenging issues for AC power systems is frequency regulation. Instantaneous power generation and consumption must match to avoid frequency deviations from the nominal value. Frequency deviations can lead to stability, safety, and power quality problems. All of this makes necessary the establishment of three regulation levels (primary, secondary, and tertiary) for frequency control purposes. Primary frequency regulation (*PFR*) is the first control response in case of frequency deviation and acts by injecting or receiving power to stabilize the frequency. Therefore, power generators must have an energy reserve to apply *PFR* whenever the frequency is outside of its permissible limits [1–3]. *PFR* service has been traditionally provided by synchronous generators; nevertheless, they have the following limitations: (1) a percentage of the available generator power must be reserved, diminishing the energy that can be sold in the spot market; (2) the response speed to

inject power can be slow; and (3) frequency regulation is indirectly performed through the generator speed regulation system and may cause power system frequency oscillations.

The use of *BESS* has been proposed as an alternative to solve the limitations of performing *PFR* service with synchronous generators. In general terms, a *BESS* is a device based on power electronics containing a storage system (batteries) and an inverter, which in turn reacts quickly and allows the provision of *PFR* service [4]. One of the benefits of using *BESS* for *PFR* service is its extremely fast response under load variations. Additionally, research on *BESS* technology is making them more robust to withstanding frequency imbalances, with more power capacity and a low self-discharge rate [5,6]. Furthermore, with the recent growth of renewable energies and micro-grids, *BESS* for *PFR* support has become an emerging line of research [5,7–10]. Due to resource intermittency, solar plants are not able to maintain an appropriate energy reserve, making *BESS* implementation necessary to accomplish *PFR* requirements. For this reason, this paper proposes a *BESS* sizing strategy for *PFR* in these types of applications.

Batteries in storage systems represent the highest equipment cost [11–13]; even more, designers usually overestimate battery sizes in *BESS* to guarantee reliability in the system incurring an unnecessary higher investment cost. For appropriate battery sizing, numerous researchers have presented optimization techniques to trade off BESS size and system reliability in operation. The work of [2] proposed the inclusion of emergency resistors to optimize *BESS* for *PFR* that must act when over-frequency events occur. The authors also exposed an algorithm to adjust the *SoC* limits. In [14], the authors illustrated a method of sizing *BESS* for isolated systems with high penetration of renewable energies; they had to face significant frequency deviations due to the lack of a highly inertial synchronous generation system. In [15], a cost-based multi-objective optimization that included the distribution system cost and the battery cycling cost was presented. In [16], a methodology for optimizing a LiFePO$_4$ battery in *BESS* that took into account the U.K. regulatory framework was reported. The main input of the methodology is frequency historical data. The work presented in [17] proposed a stochastic approach to operate a *BESS* that includes a battery degradation model to obtain the maximal battery lifetime. The paper [5] designed an optimization of a *BESS* that trades off investment and operating cost. The authors also considered keeping *SoC* within a safe range. In general terms, most of the reviewed papers formulated the problem of *BESS* sizing as a dynamic programming problem. It is basically approached from the perspective of the system operation in which an optimization model seeks the minimum operating and investment cost.

This paper proposes a holistic strategy for sizing *BESS* for *PFR* support of solar photo-voltaic plants. In addition to formulating an optimization problem for sizing *BESS*, the proposed strategy also includes a performance evaluation algorithm that emulates *BESS* operation. The optimization model mainly includes investment costs as is usually done by researchers in the reviewed papers. However, with the aim to improve *BESS* sizing results for *PFR*, a novel penalty function for *SoC* is proposed to ensure, once the *BESS* is in operation mode, that its *SoC* does not pose a risk to *PFR* service. The performance assessment algorithm is fed by the results of the optimization model, emulates *BESS* operation, and provides important performance indexes such as penalization costs, battery lifetime, battery replacements, and *SoC*. This permits making better decisions in the election of the *BESS* size. The performance assessment considers a great variety of operational restrictions and is less computationally intensive than the optimization model. This algorithm properly complements the *BESS* sizing strategy since it adds realistic operational aspects to this analysis. In summary, the main contributions of the paper are listed as: (1) a novel penalty function included in the optimization model to ensure that *SoC* does not pose a risk to *PFR* service; (2) a performance assessment algorithm that emulates *BESS* operation and permits the calculation of performance indexes such as penalization costs, battery lifetime, battery replacements, and *SoC*; and (3) a sizing strategy that is composed of the optimization model and the performance assessment algorithm; together, the inclusion of multiple *BESS* operational restrictions in the sizing process to add a realistic characterization of *BESS* in *PFR* applications is possible.

This paper is divided into the following sections: Section 2 illustrates *BESS* operation and defines operational restrictions. Section 3 proposes the optimization model to find the optimal energy capacity. Section 4 elaborates on the *BESS* performance assessment algorithm. Section 5 reports the results of applying the strategy to a given case and discusses them. Section 6 presents the most relevant conclusions of this research.

2. *BESS* Operation under *PFR*

Under *PFR*, *BESS* power is essentially a function of grid frequency, *SoC*, and frequency droop *S*. For modeling purposes, *BESS* power is split into two terms namely P_t^{PFR} and P_t^{SoC}. Both represent instantaneous power during period t; the first one is required to model the *PFR* service, whereas the latter is employed to maintain *SoC* within a target *SoC* band. Furthermore, *BESS* maximum power P_n^{BESS} is defined as a given percentage ρ of a solar power plant P_n^G, i.e., $P_n^{BESS} = \rho P_n^G$.

Figure 1a shows different operation regions regarding the droop characteristic. The horizontal axis represents grid frequency deviation Δf_t, and the vertical axis represents *BESS* power for *PFR* service P_t^{PFR}. In Figure 1a, operation regions are indicated as (1), (2), (3), (4), and (5). Regions (1) and (5) represent *BESS* power saturation, where *BESS* exchanges its maximal power P_n^{BESS} with the grid. Regions (2) and (4) represent linear operation where power is proportional to frequency deviation with a slope equal to the droop factor *S*. Finally, Region (3) is the deadband, where *PFR* is not necessary and *BESS* does not exchange power.
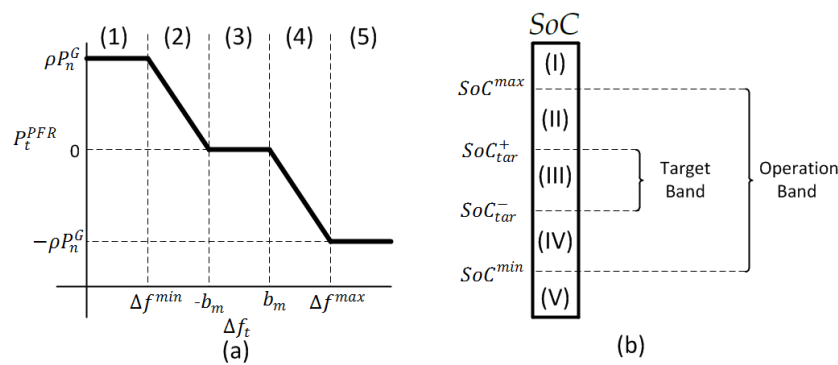

Figure 1. *BESS* operating regions: (**a**) from the droop characteristic; (**b**) from *SoC*.

BESS state of charge SoC_t is defined as the quotient between its currently-stored energy E_t and its nominal storage capacity E_n, $SoC_t = \frac{E_t}{E_n}$. Figure 1b shows *BESS* operation regions according to its SoC_t as indicated in (I), (II), (III), (IV), and (V). Region (I) represents battery overcharge, that is $SoC > SoC^{max}$, and thus, it is not possible to absorb power from the grid. Likewise, Region (V) represents battery over-discharge, that is $SoC < SoC^{min}$, and it is not possible to deliver power to the grid. Regions (II) and (IV) represent an *SoC* where it is possible to absorb and deliver power to the grid. Thus, there are no limitations in providing *PFR* service, but *SoC* is out of its target band. In Regions (I), (II), (IV), and (V), it is necessary to absorb or deliver power P_t^{SoC} to return *SoC* to its target band. Finally, *SoC* Region (III) is limited by $SoC_{tar}^- \leq SoC_t \leq SoC_{tar}^+$; no P_t^{SoC} power is needed, and *PFR* service can be provided without limitations.

Figure 2 explains how P_t^{SoC} (Figure 2a) and P_t^{PFR} (Figure 2b) powers are calculated according to the regions defined in Figure 1. It is assumed a positive sign for power delivered from *BESS* to the grid (discharge) and negative for power absorbed by the *BESS* from the grid (charge). In Figure 2b, $P_t^{PFR}(\Delta f_t)$ is the portion of power that reacts in a linear fashion with respect to frequency deviations and is given by Equation (1). A positive sign in b_m applies when frequency deviation is positive, while a negative sign applies when frequency deviation is negative.

$$P_t^{PFR}(\Delta f_t) = \frac{-1}{S \cdot f_n}(\Delta f_t \pm b_m) \tag{1}$$

Notice that P_t^{SoC} is allowed to be different from zero only when the grid frequency lies in the deadband region (3). In this sense, P_t^{SoC} can be understood as a sudden load or injection of power to the system depending on its sign. If its magnitude is not small enough, it could cause imbalance between power generation and demand, which in turn could eventually produce further frequency deviations. Therefore, to avoid these perturbations in the system, P_t^{SoC} is assumed to be at most a small percentage γ of *BESS* nominal power P_n^{BESS}.
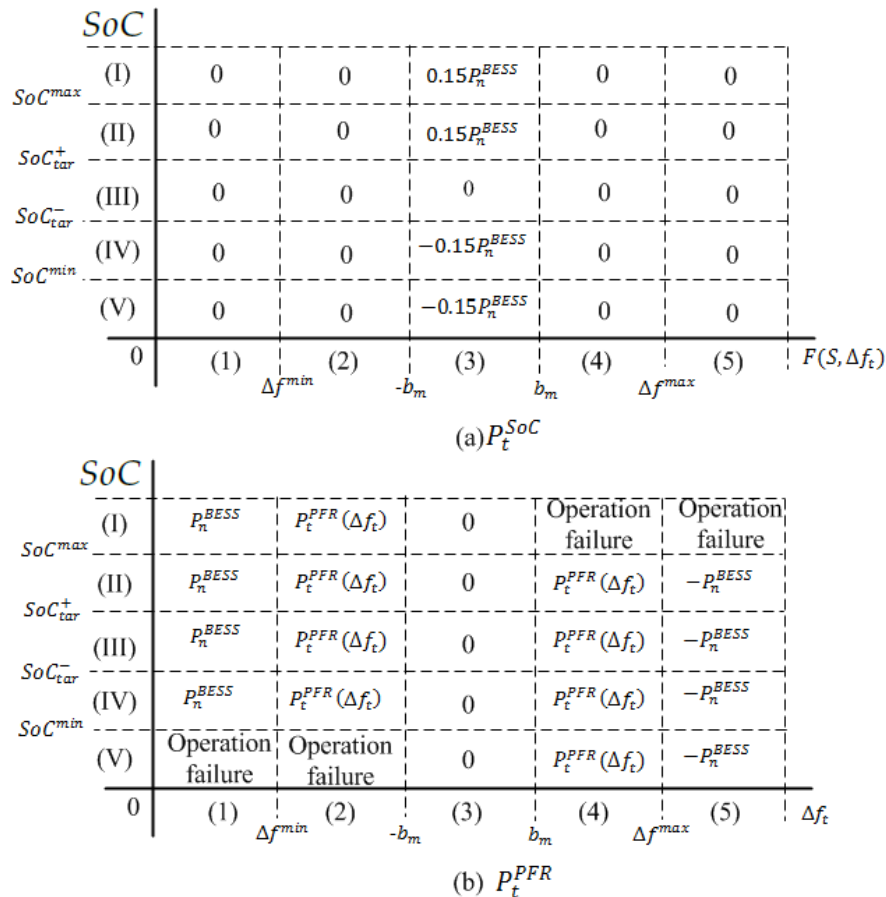
(a) P_t^{SoC}

SoC	(1) Δf^{min}	(2) $-b_m$	(3) b_m	(4) Δf^{max}	(5) $F(S, \Delta f_t)$
(I) SoC^{max}	0	0	$0.15 P_n^{BESS}$	0	0
(II) SoC_{tar}^{+}	0	0	$0.15 P_n^{BESS}$	0	0
(III) SoC_{tar}^{-}	0	0	0	0	0
(IV) SoC^{min}	0	0	$-0.15 P_n^{BESS}$	0	0
(V)	0	0	$-0.15 P_n^{BESS}$	0	0

(b) P_t^{PFR}

SoC	(1) Δf^{min}	(2) $-b_m$	(3) b_m	(4) Δf^{max}	(5) Δf_t
(I) SoC^{max}	P_n^{BESS}	$P_t^{PFR}(\Delta f_t)$	0	Operation failure	Operation failure
(II) SoC_{tar}^{+}	P_n^{BESS}	$P_t^{PFR}(\Delta f_t)$	0	$P_t^{PFR}(\Delta f_t)$	$-P_n^{BESS}$
(III) SoC_{tar}^{-}	P_n^{BESS}	$P_t^{PFR}(\Delta f_t)$	0	$P_t^{PFR}(\Delta f_t)$	$-P_n^{BESS}$
(IV) SoC^{min}	P_n^{BESS}	$P_t^{PFR}(\Delta f_t)$	0	$P_t^{PFR}(\Delta f_t)$	$-P_n^{BESS}$
(V)	Operation failure	Operation failure	0	$P_t^{PFR}(\Delta f_t)$	$-P_n^{BESS}$

Figure 2. *BESS* output power as function of *SoC* and grid frequency. (**a**) Power required for *SoC* regulation; (**b**) Power required for *PFR* service.

The proposed *BESS* operation model does not take into account limitations due to the battery charger or BMS (Battery Management System) operation. Previous works like [18,19] considered current and voltage profiles that must be met to guarantee battery safety and health during battery charge operations. Thus, power absorption can be, at certain times, limited to a value lower than that specified by P_t^{SoC} or P_t^{PFR}. These limitations are not considered in this work.

3. Proposed Optimization Model for *BESS* Sizing

The proposed optimization model is aimed to find both the best *BESS* storage capacity E_n and operation set points SoC_{tar}^{-} and SoC_{tar}^{+}. One of the criteria used to achieve satisfactory *BESS* size for *PFR* is investment cost. Thus, the authors of this paper have assembled this optimization model aimed to find both a cost-effective *BESS* size that guarantees the proper *PFR* service and *SoC* set points that guide the *BESS* operation in real time. To do so, the *SoC* dynamics, via difference equations, is modeled using short integration periods that allow capturing frequency deviation dynamics. Two of the key input parameters of the model are SoC^{min} and SoC^{max} since they allow tuning the model according to the results of the performance assessment model. It is important to clarify that the key aspects of *BESS*

that are relevant to this formulation are power exchange and energy storage. These parameters define the ability (or inability) to offer a proper *PFR* service. Although the type of battery and its associated chemistry process are relevant from a construction and design point of view, they are not part of the inputs of the proposed *BESS* sizing strategy for *PFR* purposes. The mathematical model is given by the objective function (2) and Constraints (3)–(11).

$$\text{minimize} \qquad f_0 = I \cdot E_n + \lambda \sum_{t=1}^{T} p_t, \qquad (2)$$

$$\text{subject to} \qquad p_t \geq m_1 \left(E_t - E_{tar}^+ \right), \quad \forall t = 1, \dots, T, \qquad (3)$$

$$p_t \geq (m_1 - m_2)(SoC^{max} - 0.1)E_n - m_1 E_{tar}^+ + m_2 E_t, \quad \forall t = 1, \dots, T, \qquad (4)$$

$$p_t \geq -m_1(E_t - E_{tar}^-), \quad \forall t = 1, \dots, T, \qquad (5)$$

$$p_t \geq -(m_1 - m_2)(SoC^{min} + 0.1)E_n + m_1 E_{tar}^- - m_2 E_t, \quad \forall t = 1, \dots, T, \qquad (6)$$

$$P_t^{PFR} = P_n^G \max\left(0, \min\left(\rho, \frac{-1}{S \cdot f_n}(\Delta f_t + b_m)\right)\right)$$
$$+ P_n^G \max\left(0, \min\left(-\rho, \frac{-1}{S \cdot f_n}(\Delta f_t - b_m)\right)\right), \qquad (7)$$

$$E_t = E_{tar}^- \cdot \mathbf{1}_{\{t=1\}} + E_{t-1} \cdot \mathbf{1}_{\{t \geq 1\}} + \Delta t \left(P_t^{SoC} + P_t^{PFR}\right), \quad \forall t = 1, \dots, T, \qquad (8)$$

$$E_{tar}^+ - E_{tar}^- \leq \rho_{gap} E_n, \qquad (9)$$

$$SoC^{min} E_n \leq E_t \leq SoC^{max} E_n, \quad \forall t = 1, \dots, T, \qquad (10)$$

$$|P_t^{SoC}| \leq \gamma P_n^{BESS} \mathbf{1}_{\{-b_m \leq \Delta f_t \leq b_m\}}, \quad \forall t = 1, \dots, T. \qquad (11)$$

The optimal *BESS* dimension is obtained by minimizing its investment cost and the penalty function, as shown in Equation (2). *I* represents the unitary investment cost in \$/MWh of storage capacity; thus, the product $I \cdot E_n$ is the total *BESS* cost in \$. p_t, a convex and piecewise affine function that is illustrated in Figure 3, penalizes *SoC* deviations during period *t* from its target band as described in Equations (3)–(6). m_1 and m_2 ($m_1 < m_2$) are the slopes of p_t. The set of inequalities (3)–(6) was employed to describe the convex function p_t. This is a common strategy in convex optimization formulations and can be understood as the epigraph of the function. To address additional convex optimization concepts, the interested reader can refer to the textbook [20].
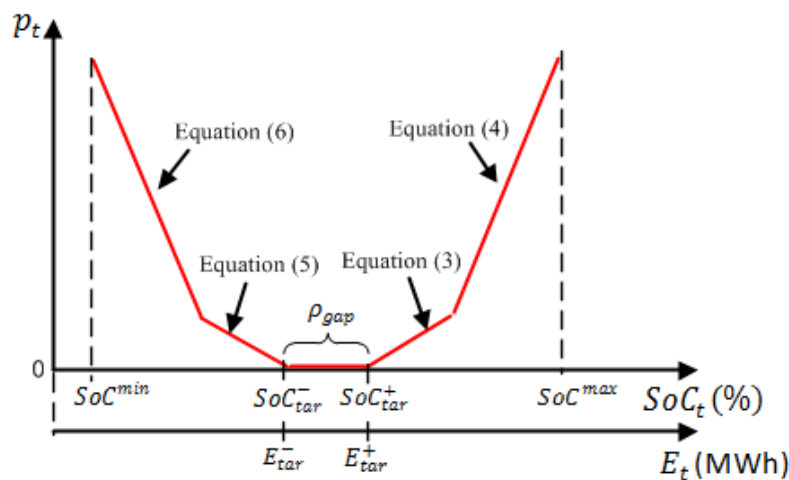

Figure 3. *SoC* deviation penalty function p_t.

Parameters SoC^{min} and SoC^{max} represent *SoC* hard limits, i.e., during the optimization, the *BESS* is not allowed to operate outside the interval $\left[SoC^{min}, SoC^{max}\right]$. Furthermore, the resulting *SoC*

target band is defined by interval $\left[SoC_{tar}^{-}, SoC_{tar}^{+}\right]$. These bounds are related to decision variables $E_{tar}^{-} = SoC_{tar}^{-} E_n$ and $E_{tar}^{+} = SoC_{tar}^{+} E_n$ (in MWh), which in turn define the lower and upper bounds of the target storage level, respectively.

As depicted in Figure 3, p_t penalizes the objective function when either $E_t < E_{tar}^{-}$ or $E_t > E_{tar}^{+}$; and p_t is even larger as long as E_t approaches either $SoC^{min} E_n$ or $SoC^{max} E_n$. In case $E_{tar}^{-} \leq E_t \leq E_{tar}^{+}$, p_t is zero. This function is constructed with the purpose of maintaining *SoC* far enough from its limits (SoC^{min} and SoC^{max}), not only in the optimization model, but also during the *PFR* assessment, as will be discussed later in Section 4.

Constraint (7) allows computing P_t^{PFR} in terms of frequency deviation Δf_t, as illustrated in Figure 1a. The slope of linear segments depends on the system frequency regulation constant (or frequency droop) S, nominal frequency f_n, deadband ($2b_m$), and P_n^G. Signal $P_t^{PFR}, t = 1, \ldots, T$ does not belong to the decision variable set, but it is a signal resulting from the power system dynamics. In general terms, P_t^{PFR} is the power for the *PFR* service and is computed such that 1 MW of power should cause a relative change in frequency S between 4% and 6% with respect to its nominal value f_n.

A stored energy update is performed according to Constraint (8). This constraint is nothing but a difference equation representing energy storage as the integral of net power handled by the *BESS*. Indicator function $\mathbf{1}_{\{x \in A\}}$ is one whenever $x \in A$, and zero otherwise. The initial condition assumes that the storage level is at E_{tar}^{-}. Energy stored E_t is updated as a result of successive charge and discharge signals throughout the analysis horizon. When $-b_m \leq \Delta f_t \leq b_m$, frequency is located in Region 3 of Figure 1a, which indicates that the *BESS* enters into either a charging or discharging process. This process is developed to return storage level E_t to the target band given by $\left[E_{tar}^{-}, E_{tar}^{+}\right]$ (this is equivalent to returning *SoC* to its target band given by $\left[SoC_{tar}^{-}, SoC_{tar}^{+}\right]$) by the proper values of $P_t^{SoC}, t = 1, \ldots, T$.

The storage target band is parameterized in Constraint (9) in terms of a percentage ρ_{gap} of storage capacity E_n. This constraint basically states that the width of the gap (measured in units of energy) cannot be larger than a small percentage of the nominal storage capacity. In any case, stored energy E_t cannot operate outside the operational limits $SoC^{min} E_n$ and $SoC^{max} E_n$ as suggested by the restrictions (10).

Power signal $P_t^{SoC}, t = 1, \ldots, T$ represents a key decision variable in this model. It allows managing *SoC* at times when frequency is under the normal condition. The constraints (11) state that P_t^{SoC} needs to be at most a percentage γ of *BESS* nominal power. Note that P_t^{SoC} can be either positive or negative, i.e., it can represent charge or discharge only when frequency deviations are small. The model chooses the magnitude of P_t^{SoC} according to the "distance" of current *SoC* to its target band during period t.

4. *BESS* Performance Assessment Algorithm

A performance assessment algorithm is proposed to emulate *BESS* operation using a predefined frequency dataset. The assessment goal is to compute performance indexes such as penalization costs, battery lifetime, battery replacements, and *SoC* target band. The outputs of the optimization model (E_n, SoC_{tar}^{-}, SoC_{tar}^{+}) represent the input parameters to the performance assessment algorithm. This algorithm is presented as a two-step process:

4.1. Step 1: Continuous SoC Estimation

The goal of this step is to estimate *SoC* and penalization counts using the entire dataset of frequency deviations. To do so, both P_t^{PFR} and P_t^{SoC} are computed using frequency deviation from the dataset, current *SoC*, and the droop characteristic, as described in Figures 1 and 2. This is analogous to restrictions (7) and (11) presented in Section 3.

Then, an energy balance (resulting from the integral of net power $P_t^{PFR} + P_t^{SoC}$) is proposed to update the stored energy at the end of period t using Equation (12).

$$E_t = E_{t-1} + (P_t^{PFR} + P_t^{SoC})\Delta t, \quad \forall t = 1,\ldots,T \tag{12}$$

Likewise, the corresponding *SoC* is updated by dividing both sides of Equation (12) by E_n as presented in (13):

$$SoC_t = SoC_{t-1} + \frac{(P_t^{PFR} + P_t^{SoC})\Delta t}{E_n}, \quad \forall t = 1,\ldots,T \tag{13}$$

To estimate *BESS* battery lifetime, E_t^{circ} needs to be calculated. E_t^{circ} is understood as the energy that has circulated in the battery up to period t, regardless whether it is caused by charge or discharge processes. It is computed using Equation (14):

$$E_t^{circ} = E_{t-1}^{circ} + \left(\left| P_t^{PFR} \right| + \left| P_t^{SOC} \right| \right) \Delta t, \quad \forall t = 1,\ldots,T \tag{14}$$

A penalization is considered whenever *SoC* is in Region (V) and frequency deviation in Regions (1) or (2), or when *SoC* is in Region (I) and frequency deviation in Regions (4) or (5). These cases represent *BESS* failing to provide *PFR* service due to either *BESS* overcharge or over-discharge, which are considered as over-frequency and low-frequency penalization, respectively. This is depicted at the bottom-left and top-right corners of Figure 2b. The number of days with at least one over-frequency penalty is represented by N^+; whereas the number of days with at least one low-frequency penalty is N^-. The process of assessing the failure-to-provide-*PFR* is carried out continuously and will finally return the total number of penalty days with at least one penalization $N = N^+ + N^-$.

4.2. Step 2: Performance Indexes' Computation

Once Step 1 has been completed, penalization costs, battery lifetime, battery replacements, and investment costs need to be computed. Given that the total number of penalization days N is valid for the analysis horizon defined by the available frequency dataset, it is necessary to extrapolate N over the solar plant's lifetime, namely N^{life}. Assuming a similar behavior for frequency and *BESS* during the solar plant lifetime, such an extrapolation is given by:

$$N^{life} = \left(\frac{T_{sol}}{T_{asm}} \right) N \tag{15}$$

where T_{sol} is the estimated lifetime for the solar plant and T_{asm} refers to the amount of time covered in the available frequency dataset. The selected criterion for computing penalization cost C^{pen} is adapted from the Colombian *PFR* regulation [21] and shown in Equation (16). It is worth mentioning that any other criterion for cost penalties when *PFR* is not properly offered can be easily assembled with this methodology.

$$C^{pen} = 2\, G_R\, \rho\, p_{pen}\, N^{life} \tag{16}$$

G_R represents the total estimated energy generation for the solar plant in a 24-h period; ρ is the percentage of *PFR* reserve for the plant; and p_{pen} is the penalization price. However, the proposed *BESS* sizing strategy in this work is flexible enough to accommodate other penalization cost criteria.

In this work, a solar plant with an installed power capacity given by P_n^G and an average capacity factor given by *CF* is assumed. *CF* is known as the ratio of total electricity generated to the maximum energy that a power plant can produce at continuous full-power operation [22]. Thus, it is the estimated average daily energy production (G_R) is given by:

$$G_R = 24\, CF\, P_n^G \tag{17}$$

BESS battery lifetime is calculated by using the energy throughput model presented in [23,24] and as presented in Equation (18):

$$T_{BESS} = \left(\frac{E^{th}}{E_T^{circ}} \right) T_{asm} \tag{18}$$

E_T^{circ} represents the battery wear during the analysis horizon time T_{asm} and refers to the the final point of the energy circulating trajectory $E_t^{circ}, t = 1, \ldots, T$ presented in Equation (14). This lifetime model assumes a given amount of energy E^{th} that the battery can exchange (during charge or discharge) before reaching its lifetime. According to the works [23,24], E^{th} can be computed from the battery manufacturer curves that represent the number of cycles C_f as a function of average depth of discharge *DoD*. However, in this paper, E^{th} is calculated using Equation (19), which corresponds to lead-acid batteries. Nevertheless, the authors of this paper do not pretend to limit the range of application of this methodology to lead-acid batteries only. For other battery technologies, E^{th} can be estimated using the approaches presented in [4,25].

$$E^{th} = DoD \, E_n \, C_f \tag{19}$$

Optimal *BESS* sizing for *PFR* purposes requires the evaluation of performance in operation. A *BESS* with low energy capacity (E_n) has low initial investment costs; but in the end, it can be more expensive if additional investment costs over the lifetime of the solar project are considered due to future replacements. Thus, for a more realistic economic evaluation, the number of *BESS* replacements N_r during the solar plant lifetime needs to be calculated. To do so, Equation (20) is employed:

$$N_r = \left\lceil \frac{T_{sol}}{T_{BESS}} \right\rceil \tag{20}$$

where $\lceil x \rceil$ indicates the least integer that is greater than or equal to x. Thus, N_r indicates how many *BESS* need to be invested in in order to fully cover the power plant's lifetime period. Finally, total *BESS* investment and replacement costs are calculated as follows:

$$C^I = I \, E_n \, N_r \tag{21}$$

The final decision regarding the optimal *BESS* size is chosen as the one that minimizes the total project cost given by $C^{pen} + C^I$.

5. Results

In order to test both the optimization model and the assessment algorithm, a $P_n^G = 10$ MW solar PV power plant with a *CF* = 20% capacity factor was considered. Lifetime was assumed to be T_{sol} = 25 years. As mentioned earlier, the *BESS* was designed entirely for providing *PFR* service to which the solar PV plant was committed. $\rho = 3\%$ of the plant capacity had to be dedicated for frequency control, which means the nominal *BESS* power was $P_n^{BESS} = 0.3$ MW. The nominal frequency was $f_n = 60$ Hz and the deadband $b_m = 30$ MHz. Furthermore, the frequency droop was $S = 6\%$. *BESS* investment cost was assumed to be $I = 600$ \$/kW; this is considering the battery management system and power conversion system. An *SoC* target bandwidth of ρ_{gap} = 5% was assumed, and slopes for the penalty function were given by m_1 = 40 and m_2 = 80. The assumed number of *BESS* cycles was C_f = 100,000. The percentage of *BESS* nominal power γ to recover its *SoC* to the target band was assumed to be 15%. Since nominal power was 300 kW, $|P_t^{SoC}|$ was bounded by 45 kW in order to prevent posterior frequency deviations.

Frequency event data were provided by the Colombian Independent System Operator (ISO) called XM. It contains 10,819,703 frequency records, sampled every four seconds by a Phasor Measurement Unit (PMU), and they were collected between December 2014 and April 2016. However,

a sample of one million data points was considered in the optimization model described in Section 3. The performance assessment algorithm used the entire set of available data.

The resulting linear program presented in Section 3 was solved using GAMS (24.4.6, GAMS Development Corporation, Washington, DC, USA) and took one hour on average using a 3.3-GHz, 64-GB workstation; whereas the performance assessment algorithm was coded using MATLAB (R2014a, Mathworks, Natick, MA, USA), and the average CPU time was 10 min.

5.1. Frequency Events' Characterization

Figure 4 illustrates the frequency deviation distribution of the data. Frequency deviations ranged between −0.48 Hz and 0.24 Hz; however, 95% of the data oscillated between −0.06 Hz and 0.06 Hz. During 70.22% of the time, the frequency lied in its acceptable range; thus, *PFR* was required 29.78% of the time. High-frequency events above the deadband were observed 12.5% of the time; whereas low-frequency events occurred 17.28% of the time. Therefore, the frequency distribution implied that *BESS* would be mostly absorbing power from the grid under *PFR* service.
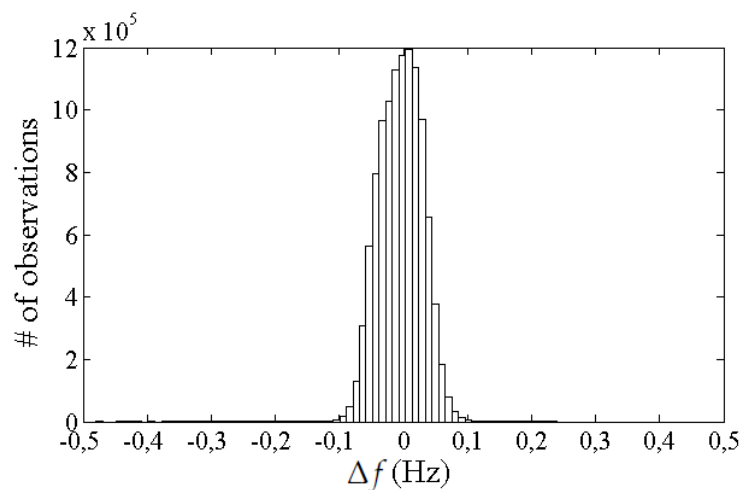

Figure 4. Δf distribution.

Data samples employed for *BESS* sizing via the optimization model represented a time window capturing the most extreme 47 days (one million data points) of frequency events. Out of these data, 47.22% of the frequency deviations required *BESS* control action for *PFR*; 18.83% and 28.39% of the frequency represented high-frequency and low-frequency events.

Figure 5a shows the P_t^{PFR} distribution resulting by employing Equation (7) to the entire dataset. The 95% confidence interval of P_t^{PFR} was $[-0.0833, 0.0833]$ MW. Figure 5b shows P_t^{PFR} for the sample frequency data. According to these distributions, both datasets were statistically similar.
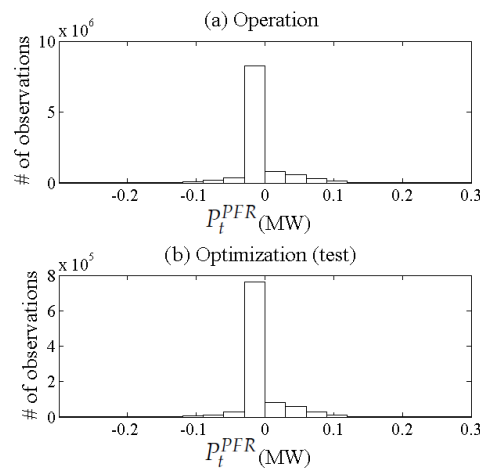
Figure 5. P_t^{PFR} distribution: (**a**) for the complete dataset; (**b**) for the optimization dataset.

5.2. BESS Sizing

The proposed optimization model was executed under different penalty levels λ and different operational parameters SoC^{min} and SoC^{max}. The optimization model provided storage capacity E_n, which is an input to the evaluation algorithm. This algorithm was useful in the sense that it performed *BESS* assessment under typical operational rules for *PFR* purposes. The *BESS* assessment was measured through the number of days in which *PFR* was not properly carried out. It was called the penalty number N, split into N^- and N^+, representing the number of penalizations in low-frequency and high-frequency events, respectively. Results are described in Table 1.

Table 1. Optimization and assessment results.

Optimization Parameters			Optimization Output			Assessment		
				Target Band (%)		N^+	N^-	N
SoC^{min}	SoC^{max}	λ	E_n (MWh)	SoC_{tar}^-	SoC_{tar}^+			
		2000	1.23	21.51	26.1	0	0	0
		1000	0.546	25.17	30.17	0	0	0
		667	0.442	27.30	32.30	0	0	0
0.10	0.90	500	0.359	29.78	34.78	0	0	0
		333	0.263	34.57	39.57	0	1	1
		60	0.135	46.68	46.68	0	1	1
		6	0.111	47.07	52.07	1	1	2
		2000	1.23	36.51	41.51	0	0	0
		1000	0.546	40.17	45.17	0	0	0
		667	0.442	42.30	47.30	0	0	0
0.25	0.75	500	0.359	44.77	49.77	0	0	0
		333	0.293	47.62	52.62	0	1	1
		60	0.254	47.15	52.15	0	1	1
		6	0.177	47.52	52.52	0	3	3
		2000	1.23	41.51	46.51	0	0	0
		1000	0.546	45.17	50.17	0	0	0
		667	0.443	47.26	52.26	0	0	0
0.30	0.70	500	0.435	47.20	52.20	0	1	1
		333	0.424	47.13	52.13	1	0	1
		60	0.373	46.96	51.96	0	1	1
		6	0.221	47.76	52.76	5	0	5

As observed in Table 1, there was a clear dependence between *BESS* size and penalty level λ. As long as λ increased, *BESS* sizing was also bigger. Penalty function p_t became more important in

the objective function (Equation (2)) whenever λ increased; then, *SoC* was less able to approach its operational limits SoC^{min} and SoC^{max} during *PFR*. To do so in practical terms, *BESS* storage capacity E_n needs to be large enough such that its energy storage level remains within the target band. The opposite occurred as long as λ decreased, since investment cost tended to prevail over penalty p_t. A graphical representation of *BESS* size vs. penalty under different *SoC* bounds is provided in Figure 6. If $\lambda > 700$, there was no perceived effect of *SoC* bounds on *BESS* size given that p_t was too large to prevail over investment cost. For lower values of λ, tighter *SoC* bounds led to bigger *BESS* sizes in order to avoid penalization during the charging and discharging process in *PFR*. These bounds are hard constraints that need to be satisfied at anytime.
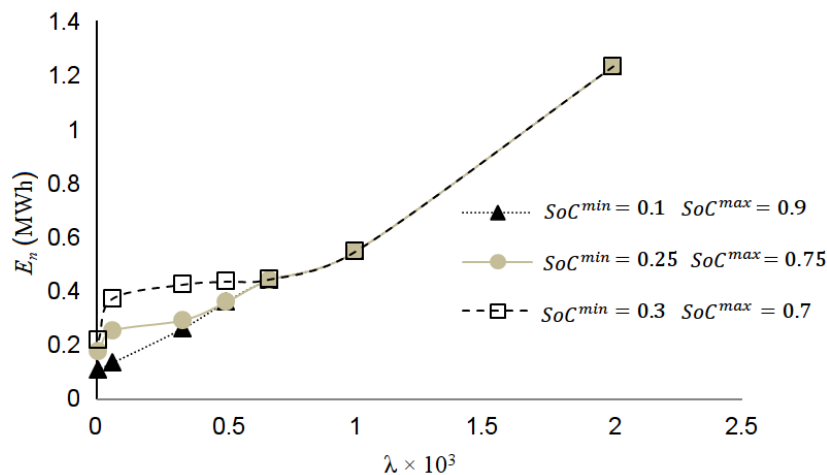
Figure 6. Nominal *BEES* energy capacity as a function of λ.

5.3. Penalization

Results in Table 1 also provide the number of penalizations caused by different *BESS* sizes. The 221-kWh *BESS* ($0.3 \leq SoC \leq 0.7$) displayed the worst performance against high frequency events, i.e., under the excess of generation in the system. This means that when sudden positive frequency deviations occurred, *SoC* was close to 70%, and *BESS* could not absorb the additional power required for *PFR*. According to the results, this situation was observed during five days in the dataset.

Additionally, the larger the *BESS* sizing, the lower the penalization levels *N*. The resulting 111-kWh *BESS* (when $\lambda = 6$) yielded one penalization in *PFR* under, both for low-frequency and high-frequency events. However, the 135-kWh/300-kW *BESS* (when $\lambda = 60$) yielded only one penalization in *PFR* under low-frequency events. *SoC* target band location also played a key role in affecting *BESS* performance. In fact, even the 359-kWh *BESS* displayed a zero penalization level when the *SoC* target band was within 29.78% and 34.78%. Indeed, as depicted in Table 1, even for a *BESS* with a fixed size E_n, *N* could change. The *SoC* target band was also a decision made by the proposed model; but, based on the findings of this work, it is essential to have an assessment tool (as described in Section 4) that provides realistic performance measures useful for determining the best *SoC* target band. The reason is that from the optimization model perspective, it is not possible to know the frequency signal in advance.

5.4. Investment Costs

In order to evaluate *BESS* investment cost, Figure 7 is presented. If *BESS* replacements were neglected, the investment costs curve would be linear with slope *I*. Figure 7 also shows how the number of *BESS* replacements N_r dramatically increased as long as E_n decreased. These results were obtained once the lifetime was computed as presented in Equations (18) and (20). In fact, if $E_n = 300$ kWh, the lifetime was four years according to the performance assessment algorithm, and thus, seven replacements are needed in order to fully provide *PFR* during the 25-year period.

This explains the increment in investment cost in Figure 7. N_r tended to increase since the charging and discharging process was more intense as long as the *BESS* size was smaller. From the total investment cost perspective, the 546-kWh *BESS* was the most cost-effective alternative. It is estimated that such a *BESS* design would require four replacements throughout the solar plant's lifetime.
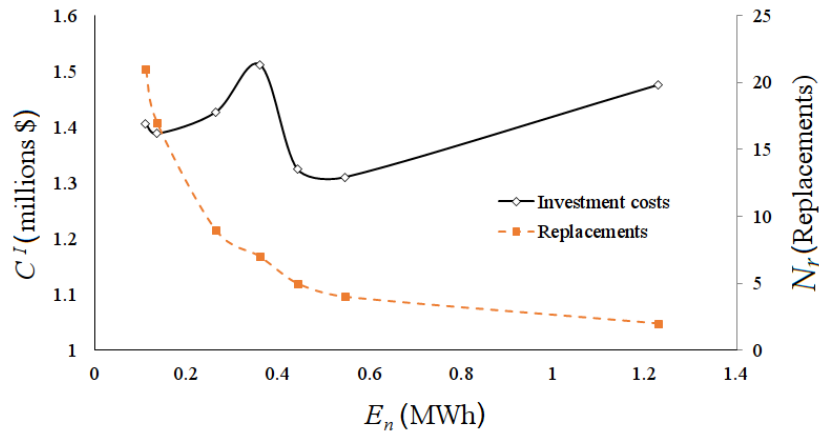

Figure 7. Total BESS investment and replacement cost.

5.5. Penalization Cost

Three scenarios of penalization cost were considered: $p_{pen} = 33.33$ $/MWh, 66.67 $/MWh, and 100 $/MWh. These represent the typical power spot price observed in the Colombian power market [26]. Penalization costs are computed once penalties (N, N^-, N^+) are found using the performance assessment algorithm presented in Section 4.

Penalization cost results are illustrated in Figure 8. A *BESS* with reduced storage capacity implies high penalization cost. For capacities around 110 kWh, the cost was over $20,000 during the 25-year period. Nevertheless, this is significantly lower—by several orders of magnitude—than the corresponding investment cost (displayed in Figure 7). An important fact is that a 546-kWh *BESS* or higher does not incur a penalization cost, i.e., this *BESS* always provides *PFR* satisfactorily.
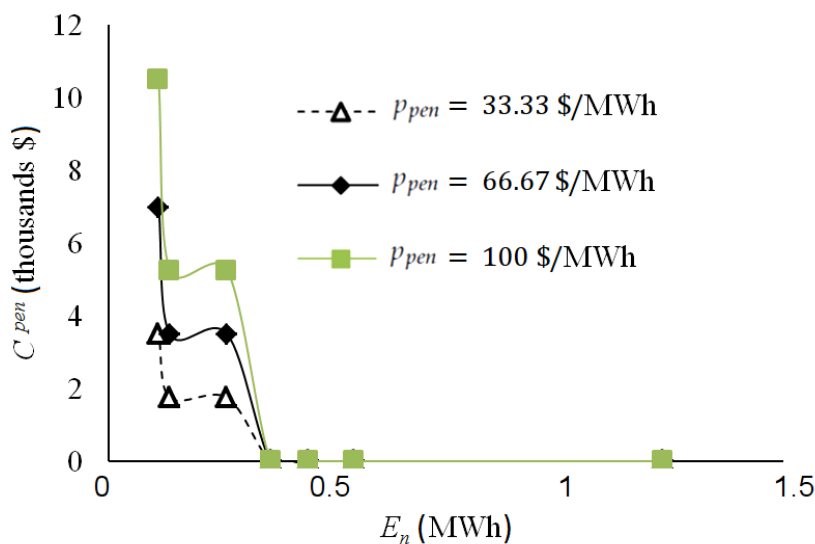

Figure 8. Penalization cost.

The *SoC* performance of the 546-kWh *BESS* under different *SoC* target bands is presented in Figure 9. Dotted horizontal lines represent the *SoC* limits (SoC^{max}, SoC^{min}), while continuous horizontal lines are the target *SoC* band limits (SoC_{tar}^+, SoC_{tar}^-). Each of these target bands are the product of the

optimization model using 47 days of data. The target band in Figure 9a is [25.2%, 30.2%], in Figure 9b is [40.2%, 45.2%], and in Figure 9c is [45.2%, 50.2%]. Based on these results, the resulting *SoC* lies most of the time in the corresponding target bands. This empirical evidence highlights the effectiveness of function p_t, which is minimized in the objective function (2).
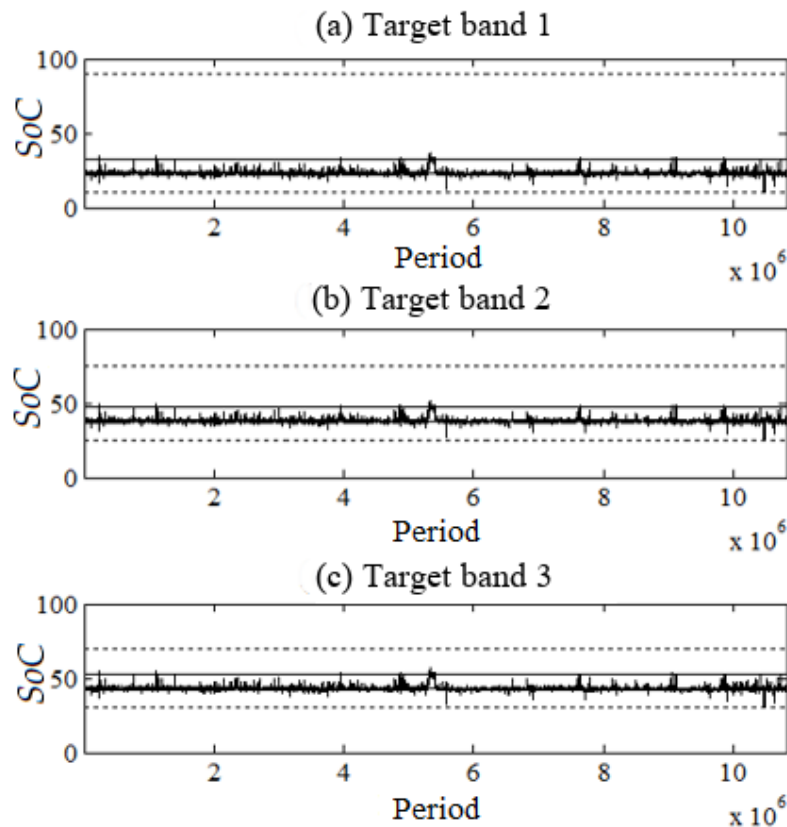

Figure 9. *SoC* trajectories for different *SoC* target bands. (**a**) [25.2%, 30.2%]; (**b**) [40.2%, 45.2%]; (**c**) [45.2%, 50.2%].

6. Conclusions

In conclusion, storage capacity, as well as operational criteria provided by the optimization model lead to significant low penalty levels when *BESS* is assessed in *PFR*. It was also found that lower and upper bounds of *SoC* impact *BESS* sizing as long as the penalty level λ decreases, the tighter the bounds, the bigger the *BESS*. The impact is negligible when λ is high. As a general remark, $\lambda > 500$ led to *BESS* designs with zero penalty levels assuming the aforementioned investment cost and parameters.

Furthermore, in order to find satisfactory *BESS* sizing alternatives, it is crucial to extract a subset of data properly—maintaining chronological order—with the most "extreme" frequency events. By doing so, not only is the optimization model lighter than the model constructed with the entire dataset, but the resulting sizing alternatives perform well in operation mode.

Additionally, in financial terms, assessing *BESS* performance during the solar plant's lifetime allows finding a better estimation of the total *BESS* investment cost. This cost should consider the number of *BESS* replacements according to the operation behavior and charge/discharge patterns, which are essentially random in *PFR*. The process of computing the number of replacements is supported by a degradation model that considers these patterns. Otherwise, the optimal *BESS* size would be smaller.

All in all, the resulting optimal *BESS* size balances investment and penalization cost under failure in supporting *PFR*. Since the operational performance was assessed with 4-s sampled data covering more than 15 months, and it is guaranteed that the optimal *BESS* size can perform satisfactorily

under a great variety of frequency disturbances. In general, the proposed methodology was carefully constructed and assembled to provide meaningful, practical, and applicable results in terms of proper size of *BESS* dedicated to providing the *PFR* service for which solar power plants are responsible. Most importantly, the proposed strategy for sizing of the *BESS* that supports *PFR* of solar power plants is simple and can be applied by industries and companies involved in the integration of renewable energy to power grids.

Abbreviations

The following abbreviations are used in this manuscript:

BESS	Battery Energy Storage System
BMS	Battery Management System
PFR	Primary Frequency Regulation
PMU	Phasor Measurement Unit
SoC	State of Charge

Nomenclature

Parameters

t	Index of periods
Δt	Sampling period (s)
I	Cost of the battery ($/ MWh)
b_m	Half of the width of the deadband (Hz)
m_1, m_2	Slopes of the penalty function p_t
SoC^{min}	Minimum state of charge (%)
SoC^{max}	Maximum state of charge (%)
SoC_{tar}^+	Upper limit for target state of charge (%)
SoC_{tar}^-	Lower limit for target state of charge (%)
SoC_t	State of charge at the end of period t (%)
ρ	Solar plant capacity percentage used for *PFR* (%)
S	Frequency regulation constant (%)
f_n	Nominal frequency of operation (Hz)
Δf_t	Frequency deviation during period t (Hz)
Δf^{max}	Maximum frequency deviation for *BESS* power limitation (Hz)
Δf^{min}	Minimum frequency deviation for *BESS* power limitation (Hz)
ρ_{gap}	Maximum percentage of target *SoC* band (%)
γ	Maximum percentage of charge/discharge during deadband frequency events (%)
P_n^{BESS}	*BESS* nominal power capacity (MW)
P_n^G	Solar power plant generation capacity (MW)
P_t^{PFR}	*BESS* power used in *PFR* during period t (MW)
P_t^{SoC}	*BESS* power used to manage *SoC* during period t (MW)
λ	Factor that varies the penalty levels
E_t^{circ}	Energy that has circulated through the *BESS* up to period t (MWh)
E^{th}	Sum of absolute energy values (charge and discharge) to reach the end of the battery life (MWh)
T	Analysis horizon (periods)
T_{asm}	Performance assessment period (years)
T_{BESS}	*BESS* estimated lifetime (years)
T_{sol}	Solar power plant estimated lifetime (years)
N_r	Number of *BESS* replacements during solar plant lifetime
N^{life}	Penalization days during solar plant lifetime

N	Penalization days during evaluation (days)
N^+	Penalization days during evaluation, due to over-frequency (days)
N^-	Penalization days during evaluation, due to under-frequency (days)
C^{pen}	Penalization costs ($)
p_{pen}	Penalization price ($/MWh)
G_R	Average daily solar energy production (MWh)
CF	Solar plant capacity factor (%)
C^I	Total *BESS* investment and replacement costs (millions $)

Decision variables

E_n	Storage capacity in MWh
E_t	Stored energy at the end of period t in MWh
p_t	Penalty function of period t
E_{tar}^+	Upper limit of the target energy band (MWh)
E_{tar}^-	Lower limit of the target energy band (MWh)

References

1. Zhou, X.; Li, W.; Li, M.; Chen, Q.; Zhang, C.; Yu, J. Effect of the Coordinative Optimization of Interruptible Loads in Primary Frequency Regulation on Frequency Recovery. *Energies* **2016**, *9*, 167. [CrossRef]

2. Oudalov, A.; Chartouni, D.; Ohler, C. Optimizing a Battery Energy Storage System for Primary Frequency Control. *IEEE Trans. Power Syst.* **2007**, *22*, 1259–1266. [CrossRef]

3. Benato, R.; Dambone Sessa, S.; Musio, M.; Palone, F.; Polito, R.M. Italian Experience on Electrical Storage Ageing for Primary Frequency Regulation. *Energies* **2018**, *11*, 87. [CrossRef]

4. Andrenacci, N.; Chiodo, E.; Lauria, D.; Mottola, F. Life Cycle Estimation of Battery Energy Storage Systems for Primary Frequency Regulation. *Energies* **2018**, *11*, 3320. [CrossRef]

5. Zhang, Y.J.A.; Zhao, C.; Tang, W.; Low, S.H. Profit-Maximizing Planning and Control of Battery Energy Storage Systems for Primary Frequency Control. *IEEE Trans. Smart Grid* **2018**, *9*, 712–723. [CrossRef]

6. Xu, B.; Oudalov, A.; Poland, J.; Ulbig, A.; Andersson, G. BESS control strategies for participating in grid frequency regulation. *IFAC Proc. Vol.* **2014**, *19*, 4024–4029. [CrossRef]

7. Tran, Q.T.T.; Luisa Di Silvestre, M.; Riva Sanseverino, E.; Zizzo, G.; Pham, T.N. Driven Primary Regulation for Minimum Power Losses Operation in Islanded Microgrids. *Energies* **2018**, *11*, 2890. [CrossRef]

8. Yan, X.; Zhang, X.; Zhang, B.; Jia, Z.; Li, T.; Wu, M.; Jiang, J. A Novel Two-Stage Photovoltaic Grid-Connected Inverter Voltage-Type Control Method with Failure Zone Characteristics. *Energies* **2018**, *11*, 1865. [CrossRef]

9. Li, J.; Ma, Y.; Mu, G.; Feng, X.; Yan, G.; Guo, G.; Zhang, T. Optimal Configuration of Energy Storage System Coordinating Wind Turbine to Participate Power System Primary Frequency Regulation. *Energies* **2018**, *11*, 1396. [CrossRef]

10. Hollinger, R.; Diazgranados, L.M.; Wittwer, C.; Engel, B. Optimal Provision of Primary Frequency Control with Battery Systems by Exploiting All Degrees of Freedom within Regulation. *Energy Procedia* **2016**, *99*, 204–214. [CrossRef]

11. Bakos, P. Life Cycle Cost Analysis for utility-scale Energy Storage systems. *J. Undergrad. Res. Univ. Ill. Chic.* **2016**, *9*. [CrossRef]

12. Chatzinikolaou, E.; Rogers, D.J. A comparison of grid-connected battery energy storage system designs. *IEEE Trans. Power Electron.* **2017**, *32*, 6913–6923. [CrossRef]

13. Luo, X.; Wang, J.; Dooner, M.; Clarke, J. Overview of current development in electrical energy storage technologies and the application potential in power system operation. *Appl. Energy* **2015**, *137*, 511–536. [CrossRef]

14. Mercier, P.; Cherkaoui, R.; Oudalov, A. Optimizing a Battery Energy Storage System for Frequency Control Application in an Isolated Power System. *IEEE Trans. Power Syst.* **2009**, *24*, 1469–1477. [CrossRef]

15. Jayasekara, N.; Masoum, M.A.; Wolfs, P.J. Optimal operation of distributed energy storage systems to improve distribution network load and generation hosting capability. *IEEE Trans. Sustain. Energy* **2016**, *7*, 250–261. [CrossRef]

16. Lian, B.; Sims, A.; Yu, D.; Wang, C.; Dunn, R.W. Optimizing LiFePO4 Battery Energy Storage Systems for Frequency Response in the UK System. *IEEE Trans. Sustain. Energy* **2017**, *8*, 385–394. [CrossRef]

17. Abdulla, K.; De Hoog, J.; Muenzel, V.; Suits, F.; Steer, K.; Wirth, A.; Halgamuge, S. Optimal Operation of Energy Storage Systems Considering Forecasts and Battery Degradation. *IEEE Trans. Smart Grid* **2018**, *9*, 2086–2096. [CrossRef]

18. Sessa, S.D.; Crugnola, G.; Todeschini, M.; Zin, S.; Benato, R. Sodium nickel chloride battery steady-state regime model for stationary electrical energy storage. *J. Energy Storage* **2016**, *6*, 105–115. [CrossRef]

19. Sessa, S.D.; Palone, F.; Necci, A.; Benato, R. Sodium-nickel chloride battery experimental transient modelling for energy stationary storage. *J. Energy Storage* **2017**, *9*, 40–46. [CrossRef]

20. Boyd, S.; Vandenberghe, L. *Convex Optimization*; Cambridge University Press: Cambridge, UK, 2004.

21. Resolución 023 de 2001. Comisión de Regulación de Energía y Gas. Available online: http://apolo.creg.gov.co/Publicac.nsf/Indice01/Resolución-2001-CREG023-2001?OpenDocument (accessed on 1 August 2018).

22. United States Nuclear Regulatory Commission: Capacity factor. Available online: https://www.nrc.gov/reading-rm/basic-ref/glossary/capacity-factor-net.html (accessed on 28 December 2018).

23. Bindner, H.; Cronin, T.; Lundsager, P.; Manwell, J.; Abdulwahid, U.; Baring-gould, I. *Lifetime Modelling of Lead Acid Batteries*; Risø National Laboratory: Roskilde, Denmark, 2005; ISBN 87-550-3441-1.

24. Beer, B.D.; Rix, A.J. Influences of Energy Throughput on the Life of Various Battery Technologies. In Proceedings of the 4th Southern African Solar Energy Conference (SASEC 2016), Stellenbosch, South Africa, 31 October–2 November 2016.

25. Xiong, R.; Li, L.; Tian, J. Towards a smarter battery management system: A critical review on battery state of health monitoring methods. *J. Power Sources* **2018**, *405*, 18–29. [CrossRef]

26. Precio de Bolsa y Escasez. Available online: https://www.xm.com.co/Paginas/Mercado-de-energia/precio-de-bolsa-y-escasez.aspx (accessed on 6 December 2018).